

# Elution Behavior for a Large Sample Size of Uranyl Ions on Reversed-Phase Columns Using $\alpha$ -Hydroxyisobutyric Acid as an Eluent

Kihsoo Joe\*, Young-Shin Jeon, Chang-Heon Lee, Sun-Ho Han, Kwang-Yong Jee, and Won-Ho Kim

Korea Atomic Energy Research Institute 150 Duckjindong, Yuseong, Taejeon, Korea 305-353

## Abstract

Large sample sizes of uranyl ions are eluted on a styrenedivinylbenzene copolymer phase and an octadecyl phase column, respectively, using  $\alpha$ -hydroxyisobutyric acid ( $\alpha$ -HiBA) as an eluent. Chromatograms are obtained from variations of the uranyl sample amounts, eluent concentrations, concentrations of the sample matrix, and the pH of the sample solution for both columns, respectively. Column capacities are estimated from the loading factors measured from the retention times of the peaks. Bandwidths of the peaks and apparent column efficiencies are measured as a function of the loading factor and calculated using the equations derived from the assumptions of a Langmuir isotherm for a single solute. Comparison between the experiment and the calculation reveals that the former showed a broader bandwidth and worse column efficiency than the latter for both columns. The two columns are compared with regards to the retention time, peak shape, column capacity, column efficiency, etc. The PRP-1 column shows a rectangular-, triangle-type peak shape, longer retention time, lower column capacity, and better column efficiency, and the LC-18 column shows a distorted Gaussian curve, shorter retention time, higher column capacity, and worse column efficiency. Column capacity, peak shape, and retention time are dependent on the eluent concentration rather than the  $\alpha$ -HiBA concentration in the sample solutions.

## Introduction

Determination of the fission products and actinide elements in spent nuclear fuels is essential for the burn-up determination and chemical characterization of the fuel. Generally, a burn-up determination by a chemical method has been performed by conventional anion-exchange chromatography for the separation of neodymium, uranium, and plutonium followed by mass spectrometry (1). However, this separation method has a shortcoming because of its time-consuming and laborious operations. Recently, high-perfor-

mance liquid chromatography has been applied to the determination of the metal elements in spent nuclear fuels for the burn-up determination or the quality control for a fuel fabrication (2,3).

For a burn-up determination, removal of the uranium matrix from the nuclear fuel solutions is required prior to an individual separation of the lanthanide as a burn-up monitor using ion chromatography. In this case, a large amount of the uranium sample solution should be injected onto the column because the neodymium content, a burn-up monitor, is very low in the sample solution compared with the uranium content. The chromatographic system using two columns connected in series was reported to have been applied for the removal of the uranium matrix on the first reversed-phase (RP) column and for the separation of the individual metal elements on the second cation-exchange column from the nuclear fuel sample solutions, respectively (4). For a burn-up determination, the maximum loading amount of uranium on the RP column would be estimated first because the neodymium amount present in the spent nuclear fuel samples is given by the sample size to be injected. Accordingly, the column capacity must be estimated in order to find the suitable loading amount of the sample.

Sadroddin Golshan-Shirazi et al. derived an analytical solution for the elution profile of the high concentration chromatographic bands on the RP column (5–7). The relation between the loading factor and a column capacity was also derived. Compared with the classic procedure for the development of analytical methods in chromatography, preparative chromatography requires a completely different approach in its implementation (7). Where a large sample size is employed, the bands become unsymmetrical; the retention time and bandwidth depend on the amount of the sample.

In this study, uranyl ions were selected as a solute for the elution behavior of a large sample size on the RP using  $\alpha$ -hydroxyisobutyric acid ( $\alpha$ -HiBA) as an eluent because this element is a major component in spent nuclear fuel samples for burn-up determinations. Two RP columns, the styrenedivinylbenzene copolymer phase (PRP-1) and the octadecyl

\* Author to whom correspondence should be addressed: email ksjo@kaeri.re.kr.

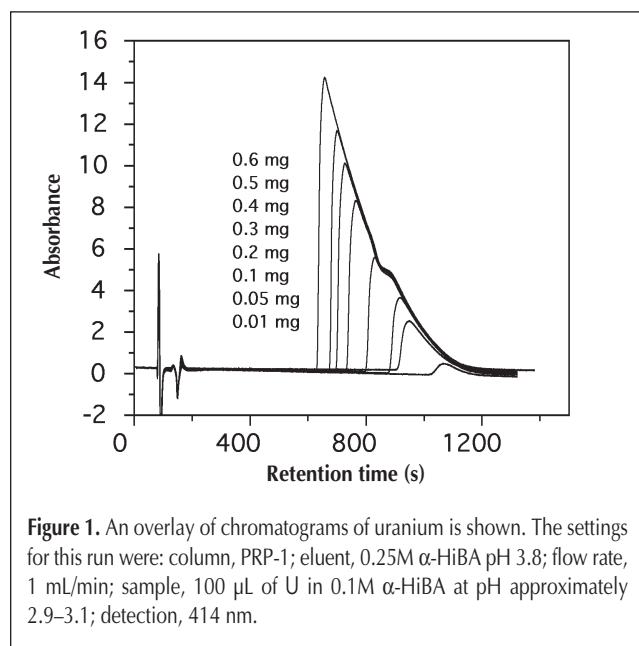
phase (LC-18), were compared in terms of the column capacity, retention time, peak shape, column efficiency, and so on to find an optimum condition for the adsorption and elution of uranyl ions on the RP because these parameters can give important information on high concentration chromatography. A large sample size of uranyl ions was injected onto the RP columns and some of the parameters mentioned previously were checked from their elution behaviors in this chromatographic run for the application of these columns to the separation of uranium and plutonium from spent nuclear fuel sample solutions.

## Experimental

### Reagent and apparatus

The chromatographic system (Metrohm, Herisau, Switzerland) consisted of a 709 IC pump, 733 IC separation center (switching valve), 812 IC injection valve, 816 IC eluent selector, 762 IC interface, and a Lambda 1010 UV-vis detector (Bishoff, Leonberg, Germany). This system was controlled by an IC Net 2.1 Metrodata software program installed in the PC (Pentium grade, Intel, Santa Clara, CA). The uranium peak was detected by absorbing 414 nm of the uranyl ion. The LC-18 column (15 × 0.46 cm, 3- $\mu$ m particle size) (Supelco, Bellefonte, PA) and the PRP-1 column (15 × 0.41 cm, 5- $\mu$ m particle size) (Hamilton, Reno, NV) were used as the RP columns.

$\mu$ -HiBA from the Aldrich Chemical Co. (Milwaukee, WI) (99%) was used as an eluent and sample medium, respectively, without further purification. The uranium working solution was prepared by the dilution of a standard solution (10000  $\mu$ g/mL, Spex Co, St. Louis, MO) to an appropriate concentration. Deionized water for all the experiments was used after treatment with the Milli-Q Water System (Millipore, Bedford, MA).



### Experimental procedure

The concentration of  $\alpha$ -HiBA as an eluent was varied from 0.025M to 0.25M to obtain the elution behavior of the uranyl ions on the RP columns. The uranyl sample solution was made as a  $\alpha$ -HiBA medium, of which the concentration ranged from 0.025M to 0.1M in order to make the uranyl HiBA complex prior to injection. A 100- $\mu$ L aliquot of uranyl sample solutions from 100–6000  $\mu$ g U/mL were injected onto the RP columns. Chromatograms were obtained, and the loading factors were measured from the retention times of the shock front of the peaks. Column capacities were estimated from the measured loading factors. The bandwidth of the peak and the apparent column efficiency were directly measured from the chromatograms, and they were also calculated from the loading factors using the equations based on a Langmuir isotherm for the elution of a single component high-concentration band.

## Results and Discussion

### Elution of the uranyl ions on the PRP-1

A neutral uranyl  $\alpha$ -HiBA complex formed between the uranyl ion and the  $\alpha$ -HiBA anion is strongly retained on the RP by the hydrophobic attraction. A large sample size of uranyl ions was eluted on the PRP-1 column using  $\alpha$ -HiBA as an eluent. Chromatograms were obtained from the variations of the uranyl sample amount,  $\alpha$ -HiBA concentration as an eluent,  $\alpha$ -HiBA concentration as a sample medium, and the pH of the sample medium, respectively. Figure 1 shows an overlay of the chromatograms obtained from the injections of the uranium solutions from 100–6000  $\mu$ g/mL onto the PRP-1 column at 0.25M  $\alpha$ -HiBA eluent and 0.1M  $\alpha$ -HiBA of the uranyl sample medium. As shown in Figure 1, the retention times of the shock front of the peaks decreased as the amount of uranium injected increased, and the peak shapes were shown as a sharp front and a long tail of a rectangular-, triangle-type. This type of peak shape is known to indicate a convex isotherm such as a Langmuir isotherm (6).

It is necessary to adjust the  $\alpha$ -HiBA concentration to the uranium concentration in a sample solution prior to injection onto the column. The maximum uranyl concentration injected was 6000  $\mu$ g/mL, which requires at least 0.05M of  $\alpha$ -HiBA in order to make a neutral compound such as  $\text{UO}_2(\text{HiBA})_2$ . In this study, two concentrations of  $\alpha$ -HiBA (0.025M and 0.1M) were selected as the sample medium, which were an insufficient and an excessive amount of  $\alpha$ -HiBA to uranyl concentration of 6000  $\mu$ g/mL for creating a neutral compound, respectively, to see how the concentration of the sample medium affects the retention behavior.

Using the equation:

$$t_f = t_o + t_p + (t_{R,0} - t_o)(1 - L_f^{1/2})^2 \quad \text{Eq. 1}$$

$$\text{Capacity} = C_{mo} V / L_f \quad \text{Eq. 2}$$

the loading factors were measured from the retention times of the shock front of the peaks as a function of the sample

amounts injected (6). Column capacities were estimated by the loading factors using equation 2 and are shown in Table I. Where,  $t_f$  is the retention time of the shock front of the peak,  $L_f$  is the loading factor,  $t_p$  is the injection time of the sample solution,  $t_{R,0}$  and  $t_0$  are the retention times of the analytical sample size and at a solvent peak, respectively.  $C_{m0}$  is the concentration of the sample injected, and  $V$  is the volume of the sample injected. At 0.25M of the  $\alpha$ -HiBA eluent, the column capacity was around 11 mg U, which was measured at the range from 0.2–0.6 mg U loaded onto the column. For the lowest loading (0.03–0.1 mg), the capacities were approximately 16–30 mg, which seems to be invalid because of the intrinsic band broadening (4). This phenomenon is similar to that of the other works performed on the C18 column (4). Figure 2 shows the chromatograms obtained at the same condition as in Figure 1 except for the 0.025M  $\alpha$ -HiBA concentration as a sample medium. Figure 2 shows similar peak shapes and retention times to those of Figure 1. However, in Figure 1 the discontinuity on the tail of the peaks was observed, and the cause of the discontinuity is not known (4). Figures 3 and 4 also show the overlays of the chromatograms obtained at 0.025M  $\alpha$ -HiBA of the eluent, and 0.1M and 0.025M  $\alpha$ -HiBA as

a sample matrix, respectively. Comparing these figures, Figure 3 also shows a similar peak shape and retention time to those of Figure 4. However, Figures 1 and 2 show quite different peak shapes compared with Figures 3 and 4. The concave and tailing in the peak shape of Figures 3 and 4 is explained because of the decreasing influence of the column efficiency on the elution profile of a large sample size with an increase of the loading factor (7) at a low concentration of the eluent, 0.025M  $\alpha$ -HiBA. In these conditions, all of the column capacities were similar (Table I) regardless of the concentration of the eluent and sample medium. This result means that the  $\alpha$ -HiBA concentration as a sample medium did not affect the peak shape and column capacity, but the eluent concentration affected the peak shape and retention time within the range of the uranium amount injected.

In Figure 5, an overlay of the peaks is shown as the variations of the pH in the sample solutions. As shown in Figure 5, the retention time decreased and the peak height increased as the pH increased, except for at pH 4.05. This phenomenon means that a more neutral complex of the uranyl  $\alpha$ -HiBA was formed as the pH increased. However, at pH 4.05 the peak height is lower, and an unknown high peak was observed at the back end of the peak, which would be auranyl hydroxide. At pH 1.84, the free uranyl ion was observed at the solvent peak position. Consequently, the optimum pH of the uranyl ions to be injected is recommended at approximately pH 3 for the maximum complexation of the uranyl- $\alpha$ HiBA compound. In Figure 6, the relationships between loading factor and retention time of the shock front of the peak and between loading factor and baseline width of the peak were shown, respectively.

As shown in Figure 6, the retention time of the shock front of the peak decreased as the loading factor increased.

Column	Mobile phase ( $\alpha$ -HiBA, pH3.8)	Sample medium ( $\alpha$ -HiBA, pH3.0)	Column capacity (mg U $\pm$ 1S)
PRP-1 (15 $\times$ 0.41 cm, 5- $\mu$ m particle size)	0.25M	0.1M	11.2 $\pm$ 0.8 (n = 5)
		0.025M	11.1 $\pm$ 1.0 (n = 5)
	0.025M	0.1M	8.9 $\pm$ 1.0 (n = 3)
		0.025M	11.2 $\pm$ 0.5 (n = 5)
LC-18 (15 $\times$ 0.46 cm, 3- $\mu$ m particle size)	0.25M	0.1M	16.0 $\pm$ 0.1 (n = 2)
		0.025M	16.2 $\pm$ 0.3 (n = 3)
	0.025M	0.1M	19.3 $\pm$ 1.6 (n = 4)
		0.025M	20.6 $\pm$ 2.5 (n = 5)

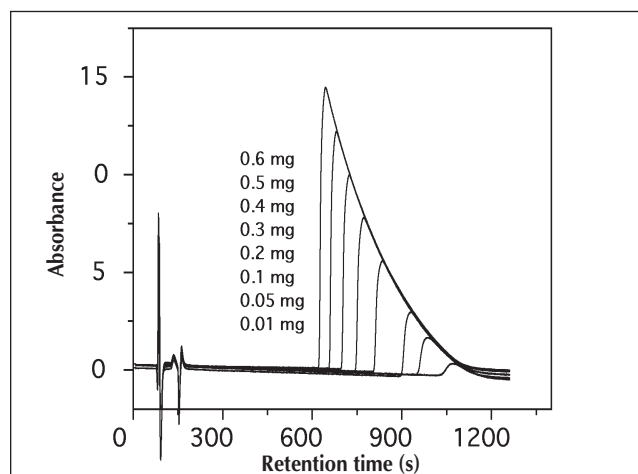


Figure 2. An overlay of chromatograms of uranium is shown. The settings for this run were: eluent, 0.25M  $\alpha$ -HiBA; sample, 100  $\mu$ L of U in 0.025M  $\alpha$ -HiBA; other conditions, same as in Figure 1.

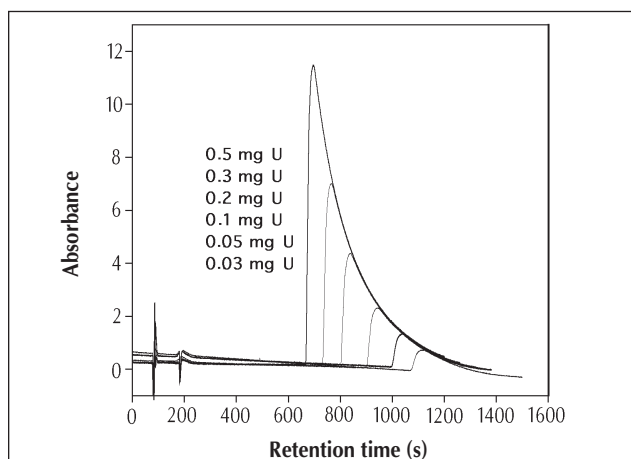


Figure 3. An overlay of chromatograms of uranium is shown. The settings for this run were: eluent, 0.025M  $\alpha$ -HiBA; sample, 100mL of U in 0.1M  $\alpha$ -HiBA; other conditions, same as in Figure 1.

This phenomenon was already observed in Figure 1. The bandwidths ( $W$ ) of the peaks were calculated using equation 3, and they were also directly measured from the chromatograms.

$$W = (t_{R,0} - t_0)(2L_f^{1/2} - L_f) \quad \text{Eq. 3}$$

The bandwidth increased as the loading factor increased for both cases. This means that the elution behavior of the uranyl ions in this chromatographic run agreed with the nonlinear chromatography, in which the retention time and the bandwidth are dependent on the amount of the sample (7).

In Figure 7, the apparent column efficiencies were plotted versus the loading factors at a condition of 0.25M  $\alpha$ -HiBA as an eluent. The column efficiency sharply increased when the loading factor was decreased from 6% down to approximately 1%, and it slowly increased when the loading factor decreased to the infinite dilution, respectively. This result is the same

phenomenon as that observed in the relationship between the bandwidth and the loading factor as shown in Figure 6. That is, the broader the bandwidth, the lower the apparent column efficiency. The calculation of the apparent column efficiency was obtained from the loading factors (6) using equations 4 and 5 at a given number, and the measurement was obtained directly from the chromatogram using equation 6. Under this condition, the limit theoretical plate number was approximately 1000 at  $k'^0 = 11.5$  with a 10- $\mu$ g sample size, which is a much lower value compared with that of the ideal model of the chromatography (6).

$$N = N_0 / (1 + 0.25 N_0 L_f) \quad \text{Eq. 4}$$

$$N_0 = 5.54 (t_{R,0} / W_{0.5})^2 \quad \text{Eq. 5}$$

$$N = 5.54 (t_R / W_{0.5})^2 \quad \text{Eq. 6}$$

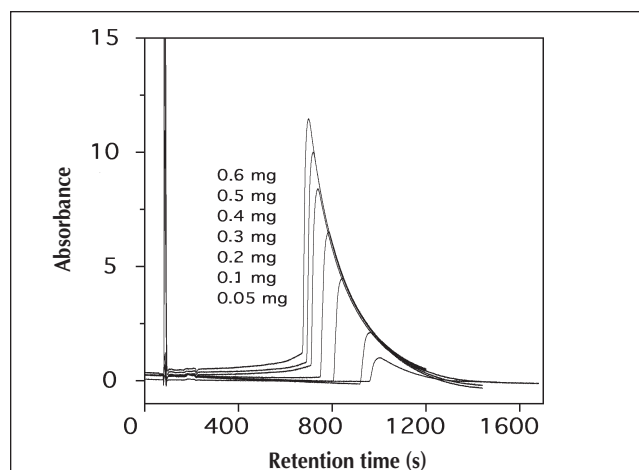


**Figure 4.** An overlay of chromatograms of uranium is shown. The settings for this run were: eluent, 0.025M  $\alpha$ -HiBA; sample, 100  $\mu$ L of U in 0.025M  $\alpha$ -HiBA; other conditions, same as in Figure 1.

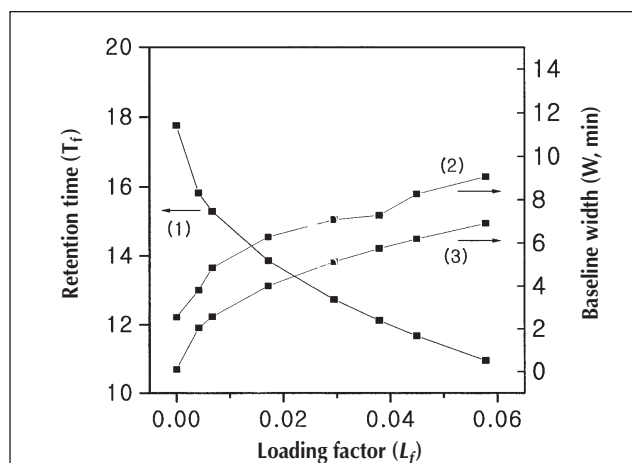


**Figure 6.** Plot of loading factor ( $L_f$ ) versus retention time ( $T_f$ ) and baseline width ( $W$ ) of the peak is shown. The settings were: column, PRP-1; eluent 0.25M  $\alpha$ -HiBA pH 3.8; flow rate, 1 mL/min; sample approximately 0.1–0.6 mg U; (1) measurement of  $T_f$ ; (2) measurement of  $W$ ; (3) calculation of  $W$ .

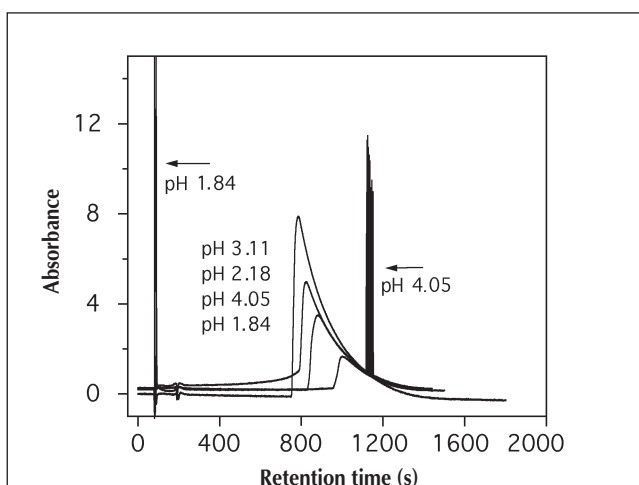


**Figure 5.** Effect of pH on the elution of uranium is shown. The settings for this run were: column, PRP-1; eluent, 0.025M  $\alpha$ -HiBA pH 3.8; sample, 100 mL of 3000  $\mu$ g U/mL in 0.05M  $\alpha$ -HiBA; pH approximately 1.84–4.05; other conditions, same as in Figure 1.

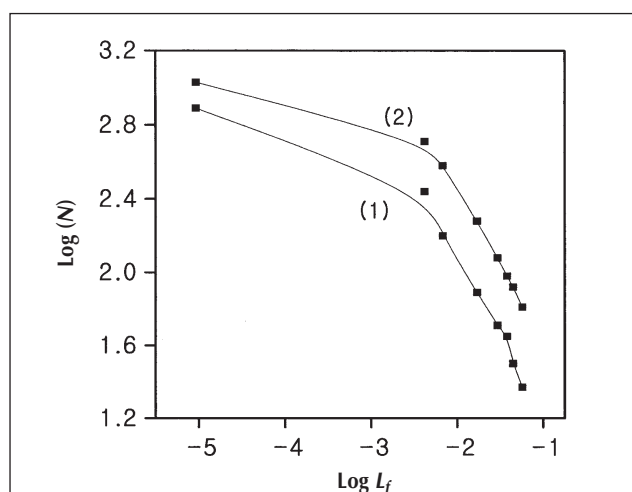


**Figure 7.** Plot of logarithm of loading factor ( $L_f$ ) versus logarithm of plate number ( $N$ ) is shown. (1) Measurement using equation,  $N = 16(T_f)/W^2$ ; (2) calculation using equation,  $N = N_0/(1 + 0.25N_0L_f)$ . Chromatographic conditions were the same as in Figure 6.

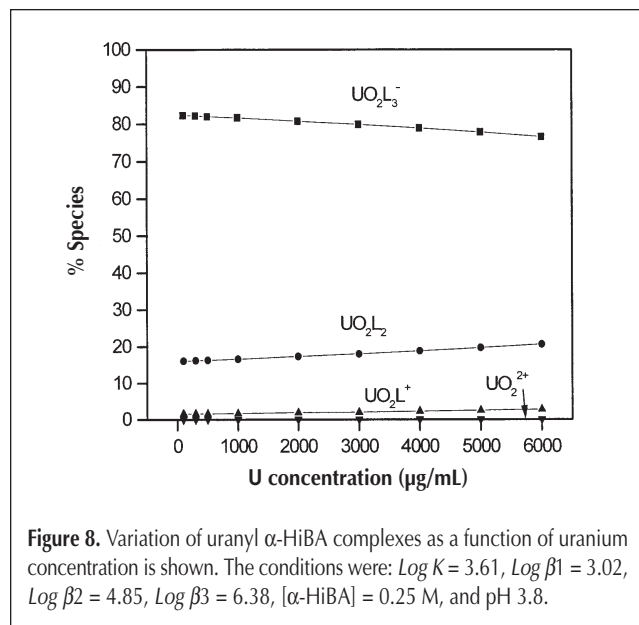


**Figure 8.** Variation of uranyl  $\alpha$ -HiBA complexes as a function of uranium concentration is shown. The conditions were:  $\text{Log } K = 3.61$ ,  $\text{Log } \beta_1 = 3.02$ ,  $\text{Log } \beta_2 = 4.85$ ,  $\text{Log } \beta_3 = 6.38$ ,  $[\alpha\text{-HiBA}] = 0.25 \text{ M}$ , and  $\text{pH } 3.8$ .

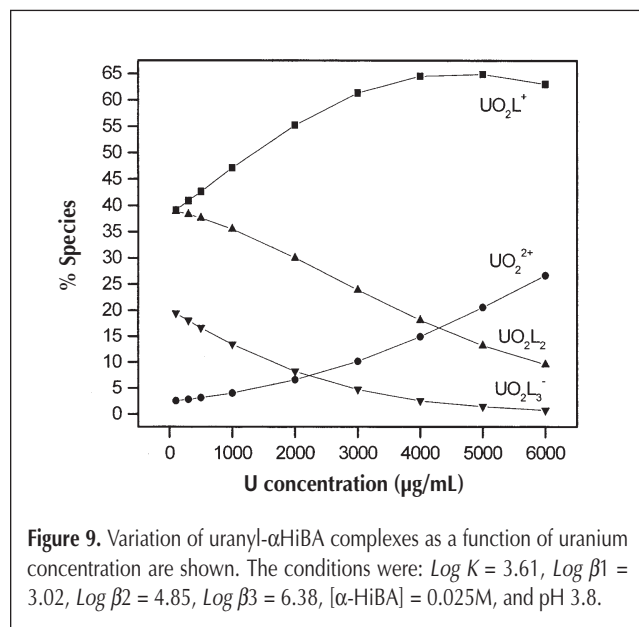


**Figure 9.** Variation of uranyl- $\alpha$ HiBA complexes as a function of uranium concentration are shown. The conditions were:  $\text{Log } K = 3.61$ ,  $\text{Log } \beta_1 = 3.02$ ,  $\text{Log } \beta_2 = 4.85$ ,  $\text{Log } \beta_3 = 6.38$ ,  $[\alpha\text{-HiBA}] = 0.025 \text{ M}$ , and  $\text{pH } 3.8$ .

As shown in Figures 6 and 7, comparisons between the experiment and the calculation revealed that the former showed a broader bandwidth, causing a worse column efficiency than the latter. The broader bandwidth in the experiment seems to be caused by the polyspecies of the uranyl  $\alpha$ -HiBA complexes such as  $(\text{UO}_2)(\text{HiBA})_2$ ,  $(\text{UO}_2)(\text{HiBA})^+$ ,  $(\text{UO}_2)(\text{HiBA})_3^-$  and  $\text{UO}_2^{2+}$  as shown in Figures 8 and 9. However, the exact reason is not identified in this study.

The neutral  $\alpha$ -HiBA compound in the eluent seems to contribute to the adsorption and compete with the uranyl  $\alpha$ -HiBA complexes on the RP. These polyspecies of the uranyl complexes also seem to compete with each other to adsorb onto the RP and cause a peak broadening. The species of the uranyl  $\alpha$ -HiBA complexes were calculated as shown in Figures 8 and 9 at the conditions of 0.25M and 0.025M of  $\alpha$ -HiBA at pH 3.8 using the stability constants (8) between the uranyl ion and the  $\alpha$ -HiBA. At a higher concentration of  $\alpha$ -HiBA (Figure 8), the neutral and the anionic complexes were largely formed, which would cause a shorter retention time and a narrower bandwidth of the peak because of the more neutral  $\alpha$ -HiBA compound in the eluent and the minor species of the uranyl  $\alpha$ -HiBA complexes, respectively, and at a lower concentration of the  $\alpha$ -HiBA (Figure 9), the cationic complexes were largely formed, which would cause a longer retention time and a broader bandwidth of the peak because of the lesser neutral  $\alpha$ -HiBA compound in the eluent and the polyspecies of the uranyl  $\alpha$ -HiBA complexes, respectively. These phenomena well agree with those observed in Figures 1–4. Accordingly, in order to explain the exact adsorption behavior of uranyl  $\alpha$ -HiBA complexes on RP, a multicomponent system should be applied (7).

The relationship between the modified loading factor  $(1 - L_f^{1/2})^2$  and the reduced capacity factor  $(k'/k'_o)$  was plotted according to equation 7, which is another expression of a dimensionless parameter for an overloaded band profile. It showed a good linearity (Table II), which agrees with the phenomenon observed at the overloaded band profile (5,6).

$$(1 - L_f^{1/2})^2 = k'/k'_o \tag{Eq. 7}$$

### Elution of the uranyl ions on the LC-18

The elution of a large amount of the uranyl ions onto the LC-18 column was also performed using  $\alpha$ -HiBA as an eluent, the same as that onto the PRP-1 column. Figures 10 and 11 show the overlays of the peaks obtained at a 0.25M  $\alpha$ -HiBA as an eluent with different concentrations of the  $\alpha$ -HiBA as the sample matrix. Figures 12 and 13 also show the chromatograms at 0.025M  $\alpha$ -HiBA eluent with 0.1M and 0.025M  $\alpha$ -HiBA as the sample matrix, respectively. The chromatograms for the LC-18 column were quite different from those obtained for the PRP-1 column (Figure 1–4). The peak shapes for the LC-18 column are distorted Gaussian curves with no steep shock front of the peaks, but the peaks for the PRP-1

**Table II. Relationship Between Loading Factor  $[(1 - L_f^{1/2})^2]$  and Reduced Capacity Factor  $(k'/k'_o)$  Obtained from the RP Columns\***

U, mg	PRP-1 (15 x 0.41 cm, 5 $\mu\text{m}$ )		LC-18 (15 x 0.46 cm, 3 $\mu\text{m}$ )	
	$k'/k'_o$	$(1 - L_f^{1/2})^2$	$k'/k'_o$	$(1 - L_f^{1/2})^2$
0.01	1	1	1	1
0.03	0.9467	0.9403	0.9544	0.9291
0.05	0.9101	0.9037	0.9165	0.8911
0.1	0.8574	0.8510	0.8734	0.8485
0.2	0.7707	0.7643	0.7595	0.7355
0.3	0.6984	0.6979	0.6810	0.6574
0.4	0.6543	0.6579	0.6304	0.6080
0.5	0.6163	0.6193	0.5975	0.5754
0.6	0.5758	0.5781	0.5494	0.5276

\* Eluent; 0.25M  $\alpha$ -HiBA, pH 3.8, Sample; 100  $\mu\text{L}$  of U in 0.1M  $\alpha$ -HiBA, pH 3.0.

column showed the rectangular, triangle types. The retention times for the LC-18 column were also much shorter than those for the PRP-1 column. The different phenomenon between the two columns for the peak shape and retention time seems to come from the different column properties, such as the chemical structure and particle size of the RP, which showed different retention behaviors for the uranyl complexes with regards to the column capacity, column efficiency, hydrophobicity, etc. The retention time decreased with an increasing of the loading factor and was shorter than that for the PRP-1 column.

Comparing the figures obtained for the LC-18 column, Figures 10 and 11 are similar in peak shape and retention time, and Figures 12 and 13 are also similar while Figures 10 and 11 are different from Figures 12 and 13 in the peak shape and retention time. In Figures 10 and 11, the shock front of the peak is higher than the rear top of the peak at the low loading

factors, and soon it is surpassed in height by the rear top of the peak as the loading factor increases, but in Figures 12 and 13, the front peak is always higher than the rear top of the peak when the loading factor is increased. This phenomenon is presumed to come from the length of the retention times. That is, at shorter retention times (Figure 10 and 11), the rear top of the peak is higher, and at longer retention times (Figures 12 and 13), the front peak is higher than the rear top of the peak. The distorted Gaussian peak for the LC-18 column seems to be because of the solvent effect [i.e., the solvent, a neutral  $\alpha$ -HiBA, competes with the solute (uranyl  $\alpha$ -HiBA complexes) on the RP column (7)].

The column capacities were also measured by the same method as for the PRP-1 column. The result showed that a higher capacity ( $\sim 20$  mg) was obtained at a lower concentration of the eluent, 0.025M  $\alpha$ -HiBA, though at a higher concentration of the eluent, 0.25M  $\alpha$ -HiBA, a lower capacity ( $\sim 16$  mg)

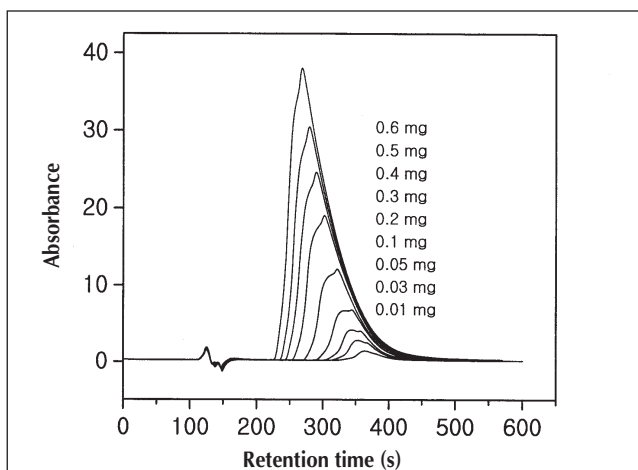


**Figure 10.** An overlay of chromatograms of uranium is shown. The conditions were: column, LC-18; eluent, 0.25M  $\alpha$ -HiBA pH 3.8; flow rate, 1 mL/min; sample, 100 mL of U in 0.1 M  $\alpha$ -HiBA at pH approximately 2.9–3.1; detection, 414 nm.

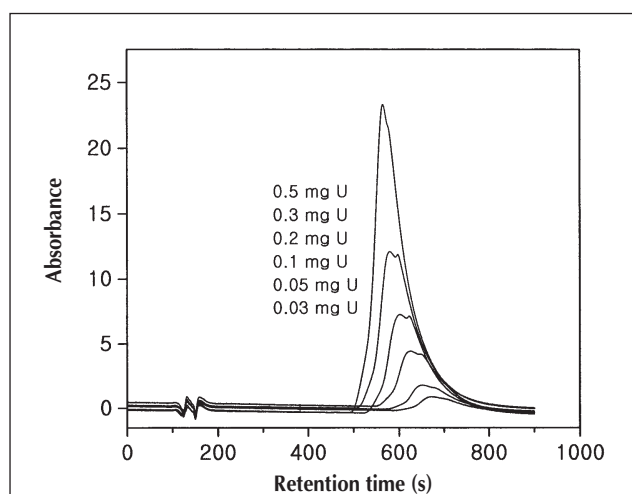


**Figure 12.** An overlay of chromatogram of uranium is shown. The conditions were: eluent, 0.025M  $\alpha$ -HiBA; sample, 100 mL of U in 0.1M  $\alpha$ -HiBA; other conditions, same as in Figure 10.

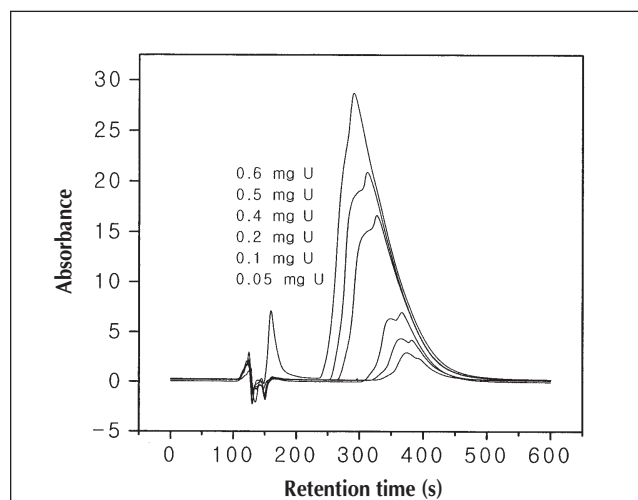


**Figure 11.** An overlay of chromatograms of uranium is shown. The conditions were: sample, 100 mL of U in 0.025M  $\alpha$ -HiBA; other conditions, same as in Figure 10.

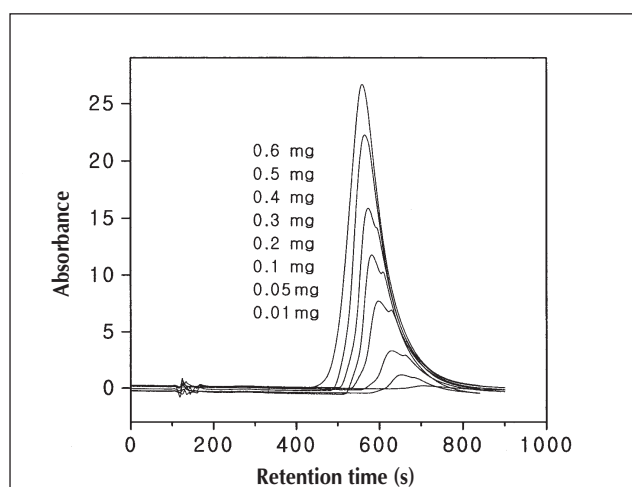


**Figure 13.** An overlay of chromatogram of uranium is shown. The conditions were: eluent, 0.025M  $\alpha$ -HiBA; sample 100 mL of U in 0.025M  $\alpha$ -HiBA; other conditions, same as in Figure 10.

was obtained (Table I). This phenomenon means that the capacity may decrease as the  $\alpha$ -HiBA concentration of the eluent increases, because the neutral  $\alpha$ -HiBA compound increases and competes with the uranyl  $\alpha$ -HiBA complexes on the RP as the  $\alpha$ -HiBA concentration of the eluent increases. Accordingly, at the condition of 0.025M  $\alpha$ -HiBA as an eluent, the injection amount of the sample solution can be increased up to 4 mL of 5,000  $\mu$ g U/mL. The LC-18 column showed a higher capacity compared to the PRP-1 column. Figure 14 shows an overlay of the chromatograms obtained at different pHs for the LC-18 column. The peak shapes were different from those for the PRP-1 column (Figure 5). The peak height, bandwidth, and retention time for the LC-18 column are higher, narrower, and shorter, respectively, than those for the PRP-1 column.

In Figure 15, the relationships between the loading factor,

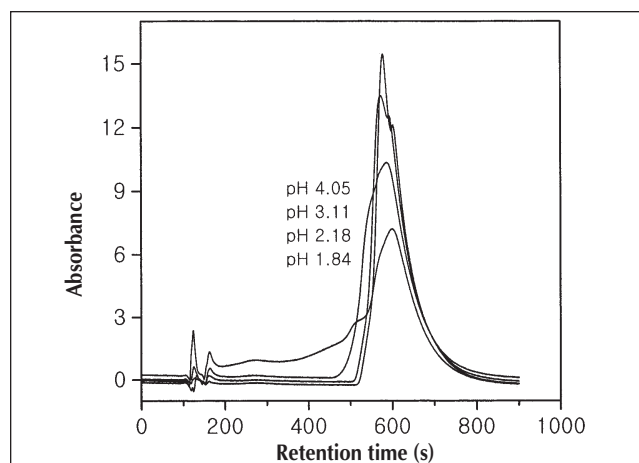


**Figure 14.** Effect of pH on elution of uranium is shown. The conditions were: column, LC-18; eluent, 0.025 M  $\alpha$ -HiBA pH 3.8; sample, 100 mL of 3000  $\mu$ g U/mL in 0.05M  $\alpha$ -HiBA; and other conditions, same as in Figure 10.

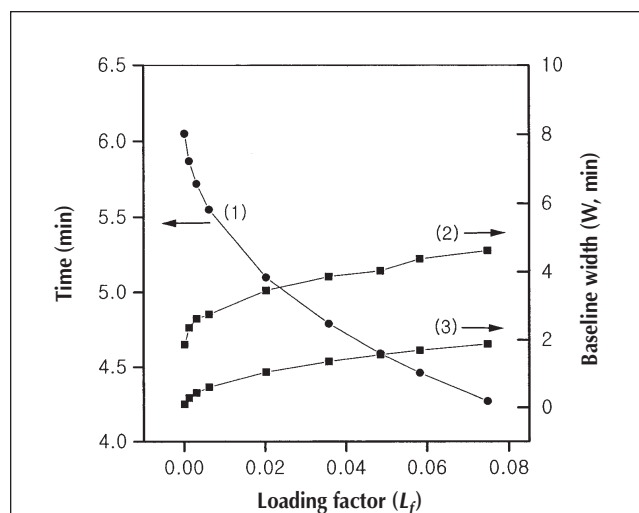


**Figure 15.** Plot of loading factors versus retention time and baseline widths of the peak is shown. The conditions were: column, LC-18; eluent, 0.25M  $\alpha$ -HiBA pH 3.8; flow rate, 1 mL/min; sample approximately 0.01–0.6 mg U; (1) measurement of  $T_f$ ; (2) measurement of  $W$ ; and (3) calculation of  $W$ .

the retention time of the shock front of the peak, and the bandwidth are plotted, respectively, and in Figure 16, the relationship between the logarithm of the loading factor and the logarithm of the column efficiency were also plotted. The retention time decreased, and the bandwidth of the peak increased as the loading factor increased. This phenomenon is also the same as that for the PRP-1 column. The calculation of the apparent column efficiency was also performed from the loading factors using equation 4 at a given number, and the measurement was also directly obtained from the chromatograms using equation 6. The experiment showed a worse column efficiency than the calculation for the same as that for the PRP-1 column. The broader bandwidth in the experiment also seems to be caused by the polyspecies of the uranyl  $\alpha$ -HiBA complexes as mentioned before for the PRP-1 column. The relationship between the modified loading factor  $(1-L_f^{1/2})^2$  and the reduced capacity factor  $(k'/k_o')$  also showed a good linearity (Table II), which is the same as that for the PRP-1 column except for the lowest loading factor.

### Conclusion

The LC-18 column showed a higher capacity, shorter retention time, and worse column efficiency than the PRP-1 column. Column capacity, peak shape, and retention time were dependent on the  $\alpha$ -HiBA concentration of the eluent not on the sample medium. A rectangular, triangle-type and a distorted Gaussian curve observed on each column, respectively, indicates that the elution of a large sample size of the uranyl ions on the RP columns follows the Langmuir adsorption behavior. The lower column efficiency in the experiment seems to be because of the multispecies of the uranyl complexes formed between the uranyl ion and the  $\alpha$ -HiBA. The different phenomena observed between the two RP columns seem to be

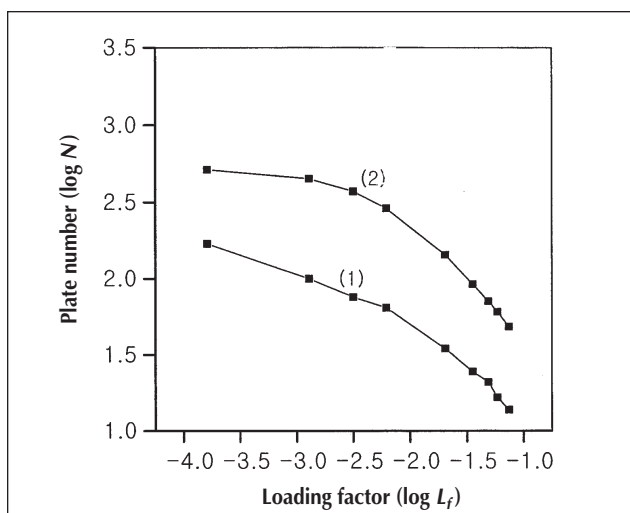


**Figure 16.** Plot of logarithm of loading factors versus logarithm of plate number is shown: (1) measurement using equation,  $N = 16(T_f)/W^2$ ; (2) calculation using equation,  $N = N_o/(1 + 0.25N_o L_f)$ ; and other conditions, same as in Figure 15.

because of the different chemical and physical properties of the RP materials.

In the future, the elution mechanism for the multicomponents of a high concentration band will be studied. The results obtained from this work will be applied to the separation of actinides in the spent nuclear fuel sample solutions.

## Acknowledgments

This study was performed as a part of the Long- and Mid-term Nuclear R&D Programs funded from the Ministry of Science and Technology of Korea. The content of this manuscript was presented as a poster at Pittcon 2004 (Chicago, IL).

## References

1. American Society for Testing and Materials. Standard method for atom percent fission in uranium and plutonium fuel (neodymium-148 method). ASTM E 321-96 (1996).
2. C.H. Knight, R.M. Cassidy, B.M. Recoskie, and L.W. Green. Dynamic ion exchange chromatography for determination of number of fissions in thorium-uranium dioxide fuels. *Anal. Chem.* **56**: 474–78 (1984).
3. S. Elchuk, K.I. Burns, R.M. Cassidy, and C.A. Lucy. Reversed-phase separation of transition metals, lanthanides and actinides by elution with mandelic acid. *J. Chromatogr.* **558**: 197–207 (1991).
4. C.A. Lucy, L. Gureli, and S. Elchuk. Determination of trace lanthanide impurities in nuclear grade uranium by coupled-column liquid chromatography. *Anal. Chem.* **65**(22), 3320–25 (1993).
5. S. Golshan-Shirazi and G. Guiochon. Experimental characterization of the elution profiles of high concentration chromatographic bands using the analytical solution of the ideal model. *Anal. Chem.* **61**: 462–67(1989).
6. S. Golshan-Shirazi and G. Guiochon. Analytical solution for the ideal model of chromatography in the case of a Langmuir isotherm. *Anal. Chem.* **60**: 2364–74 (1988).
7. G. Guiochon, S. Ghodbane, S. Golshan-Shirazi, Jun-Xiong, A. Katti, B.-C. Lin, and Z. Ma. Nonlinear chromatography: recent theoretical and experimental results. *Talanta* **36**(1-2): 19–33 (1989).
8. A.E. Martell and R.M. Smith. "Organic including macromolecular ligands", Part II. In *Stability Constants of Metal Ion Complexes*. The Chemical Society, Burlington House, London, U.K., 1971, pp. 324–25.

Manuscript received May 5, 2004;  
revision received November 19, 2004.